Alganash, B., Paul, M.C., and Watson, I.A. (2013) Investigation of heterogeneous combustion processes of biomass. In: 6th European Combustion Meeting, 5-8 Jun 2013, Sweden.

Copyright © 2013 The Authors

A copy can be downloaded for personal non-commercial research or study, without prior permission or charge

Content must not be changed in any way or reproduced in any format or medium without the formal permission of the copyright holder(s)

When referring to this work, full bibliographic details must be given

http://eprints.gla.ac.uk/81796

Deposited on: 01 July 2013

Enlighten – Research publications by members of the University of Glasgow
http://eprints.gla.ac.uk

Modelling of Heterogeneous Combustion Processes of Biomass

Blaid Alganash, Manosh C. Paul*, Ian A. Watson

Systems, Power & Energy Research Division, School of Engineering, University of Glasgow

Glasgow G12 8QQ, UK

Abstract

Results of modelling the combustion of biomass in two different chambers are presented. The combustion occurs under turbulent flow conditions for which a RANS based k-ε turbulence model is applied, while the rates of the heterogeneous reaction are defined by the chemical kinetics based on the Arrhenius equation. In the first model, a two-phase computational modelling based on the Euler-Euler approach is performed to investigate the heterogeneous combustion processes of biomass in solid carbon phase inside a newly designed combustion chamber. A transient simulation was carried out for a small amount of carbon powder situated at the cup which is located at the centre of the combustion chamber. A heat source is provided to initiate the combustion with the air supplied by three injection nozzles. The results show that the combustion is sustained in the chamber, as evidenced by the flame temperature. In the second case, an axisymmetric combustion model based on the Euler-Lagrange approach is formulated to model the combustion of pulverized coal. The predicted results show that the combustion inside the reactor is affected by the particle size and have good agreement with experimental data.

Introduction

There has been a gradual transition globally to the carbon-neutral fuels to potentially reduce global warming and at the same time the dependency on the traditional carbon-based fuels such as coal, oil, and natural gas which are facing the risk of depletion. The supply of energy has been dominated by fossil fuels for decades, and currently almost 80% of the world energy is produced from fossil based fuels [1-3]. About 10% of the world energy consumption is covered by biomass [2], which is one of the vital renewable sources of energy amongst other renewable energy sources such as wind, solar, hydro and geothermal.

The interest in using biomass fuels for energy production purposes across the world has been growing and it is considered to be one of the options to replace fossil fuels which cause the emissions of greenhouse gases [4, 5]. Particularly, the interest in using biomass for producing energy within the European Union (EU) has strongly increased, and the EU has set a target to produce at least 20% of its energy from renewable sources by 2020. Nussbaumer [6] gives an overview of combustion technologies applied in Europe today with regulations on emissions and fundamentals of combustion of wood. Moreover, possible direct combustion and an option of co-firing and gasification of biomass make it more attractive source of fuels for power production. However, a detailed study of complex and complicated combustion reactions of biomass requires a highly scientific focus, since the biomass, in general terms, includes all materials derived from photosynthetic plants and animal wastes. The sources also include naturally grown forests, energy plantations, herbaceous plants or grasses, by-products from different industries as agricultural, food, wood processing, manures, and paper industries or as municipal solid waste.

Chemical compositions and molecular structures found in any carbonaceous fuel, such as coal and biomass, are very complex. The main elements present in biomass, determined by ultimate analyses, are carbon (C), hydrogen (H), oxygen (O) and nitrogen (N) atoms. Taking into account that the C and H contents are normally greater than O and N the material is usually combustible and therefore forms a potential source of energy. Other elements also found in biomass composition are sulphur, chloride and other impurities.

The overall aim of this study is to obtain a deeper understanding about the processes of biomass combustion and to analyse various ignition methods leading to improved performance of combustion by applying computational fluid dynamics (CFD) techniques. Two different combustion models will be simulated, and particularly the objectives are to investigate the characteristics of biomass particles at different operating conditions and interactions between the gas and solid phases using multiphase methods (Euler-Lagrange and Euler-Euler).

Combustion mechanisms and Chemical reactions

There are four well-defined steps that could describe the process of solid fuel combustion process including drying, devolatilization, volatile combustion and char oxidation. Once the fuel particle enters the combustion chamber, they are heated up and the drying process (the release of moisture) occurs and the devolatilization process (the release of volatiles) occurs immediately. Then, the volatile combustion occurs leaving a char residue which combusts as well.

The burnout of solid char takes place through the heterogeneous combustion and gasification of solid char. It is governed by the diffusion of oxidizers (O_2, CO_2, H_2O) to the carbon surface and by surface reaction kinetics. Char burnout takes place between species in different phases. It usually takes place after the

* Corresponding author: Manosh.Paul@glasgow.ac.uk

devolatilization process has finished. After the component of volatiles in the particle is completely evolved as mentioned above, solid phase reactions begin. This is due to the fact that blowing volatiles through the char surface prevents oxygen from reaching char.

Char combustion involves an interaction of heterogeneous and homogeneous reactions coupled with transport limits. It is relevant to the combustion of pulverized fuels and extensive research conducted regarding this has been summarised in the review articles [7-11].

During combustion of char particles, oxygen is transported from the bulk flow to its external surface either by diffusion or convection. The combustion of char takes place only when oxygen is available, provided that the temperature in the combustion region is sufficiently high for ignition. It is enough to take into account only char combustion with oxygen and neglect char gasification rates by means of H_2O and CO_2 [7]. There is a thin layer surrounding the char particle where the homogeneous reactions occur. Through this layer, the diffusion of gaseous reactants and the products take place. The reactants diffuse into the char surface and the products diffuse away to the gaseous phase. The single-film model [12, 13] and the two-film model [14] are the most basic and simplified models. The former one assumes that either CO_2 or CO is the product of the heterogeneous reaction, and any CO produced is oxidized in the gaseous phase. The other one assumes that the carbon reacts with CO_2 and the produced CO reacts with oxygen away from the particle surface in the boundary layer. As a result of that, no oxygen reaches the particle surface.

The char produced through the volatilization process is consumed by heterogeneous reactions of combustion and gasification. Char combustion yields carbon monoxide (CO) and carbon dioxide (CO_2) according to the following reactions:

$$C(s) + O_2 \rightarrow CO_2 \quad (1)$$
$$C(s) + 0.5\,O_2 \rightarrow CO \quad (2)$$
$$C(s) + CO_2 \rightarrow 2CO \quad (3)$$

Reactions (1) and (2) are exothermic and occur very rapidly but reaction (3) is endothermic. In general, the dominating heterogeneous reaction is related to whether the char combustion rate is limited by either the diffusion of oxygen through the boundary layer surrounding the particle or the kinetic rate of the carbon oxidation reactions. Moreover, CO is expected to dominate when the temperature is high [15].

Investigations by Arthur [16] showed that the composition of the products is determined by the surface temperature. The product is entirely CO for temperatures above 1273K and the heterogeneous reactions could also include the following endothermic reaction:

$$C(s) + H_2O \rightarrow CO + H_2 \quad (4)$$

The carbon monoxide (CO) and hydrogen (H_2) resulting from reactions (2) and (4) are incorporated to the gas phase and oxidized to CO_2 and H_2O according to the following homogeneous reactions:

$$CO + 0.5\,O_2 \rightarrow CO_2 \quad (5)$$
$$H_2 + 0.5\,O_2 \rightarrow H_2O \quad (6)$$

The pulverized coal combustion model proposed in this simulation involves devolatilization, volatile combustion, char combustion and other gas phase reactions. Regarding the devolatilization, the single rate model is applied:

$$coal \xrightarrow{k} volatile\ (\alpha) + char\ (1-\alpha) \quad (7)$$

Further details on the reactions rates and coefficients are given in Alganash *et al.* [17].

Chemistry of pulverised coal

The simulations of pulverised coal combustion have been carried out on a bituminous coal. The proximate and ultimate analyses are shown in Table 1. The formulation of the coal used in the model has been simplified to a form that makes the numerical simulations simpler. The content of Sulphur (S) and Nitrogen (N) has been eliminated from the ultimate analysis. The dry ash free (DAF) composition of coal is 86.32% C, 5.36% H and 8.32% O. The elemental composition of volatile and formation enthalpy are determined from the proximate and ultimate analysis data of the coal. The volatile has the simplified molecular formula $CH_{3.392}O_{0.33}$ and a molecular weight of 20.672 kg/kmol.

Table 1: Coal analysis data

	Proximate analysis (wt%, raw basis)				Ultimate analysis (wt%, raw basis)				
	Moisture	Volatile	Fixed carbon	Ash	C	H	O	N	S
Coal	1.57	30.46	62.87	6.67	78.9	4.9	7.6	1.3	0.6
HHV = 35084.16 KJ/Kg			LHV = 33930.32KJ/Kg						

Governing equations and numerical methods

Reynolds-averaged Navier-Stokes (RANS) equations comprising the conservation of mass, momentum, energy and concentration of species are solved with a standard two-equation k-ε turbulence model for the gas phase. Such equations are Eulerian ones and solved for velocity, pressure, temperature, species mass fractions, turbulence kinetic energy and turbulence dissipation energy at every point of the computational domain. However, in the Lagrangian approach, the trajectory of discrete phase particles is determined by solving its equations of motion in the particle phase [18]. The P-1 radiation model is employed for the heat transfer of radiation with a cell based WSGGM (weighted-sum-of gray-gases model) to calculate the absorption coefficient of the gas phase. The turbulence chemistry interaction model used in the simulation is the finite/eddy dissipation model.

Fluent [18] uses an implicit finite volume method to discretise the conservation equations with a pressure-

velocity coupling derived by the SIMPLE (Semi-Implicit Method for Pressure linked equations) algorithm. The discretisation process is second order upwind scheme and the evaluation of gradients and derivatives is carried out by Green-Gauss cell based Gradient Evaluation method. For getting a stable solution, the relaxation factors have been adjusted and the residual for all the variables converged to 10^{-4} but for the energy and radiation to 10^{-6}. Boundary as well as relevant operating conditions used in the numerical simulations is described in the sections below.

Combustion Model 1

The geometry of the newly designed combustion chamber is shown in Fig. 1 (a) which consists of a small cup located in the centre of the chamber. Solid carbon particles are placed in the cup for the dispersion of carbon particles and the air is supplied through the three injection nozzles as shown in Fig. 1(b). The geometry was created by using solid works which was then exported to the pre-processor gambit to generate the mesh and specify the boundary conditions (Fig. 1b).A grid-refinement test was carried out by sequentially increasing the number of control volumes inside the chamber and the results presented are with 474748 cells and proved to be independent to the grid resolution.

For the boundary conditions, the velocity-inlet was selected with an air inlet velocity of 1m/s. The pressure outlet was selected at the outlet of the chamber as shown in Fig. 1 (b) and the walls are stationary with no-slip condition. The combustion simulations were performed for the three different particle sizes with an average diameter of 0.5mm, 1mm and 2mm respectively. An unsteady-state solver with a time-step of 10^{-3}s is used.

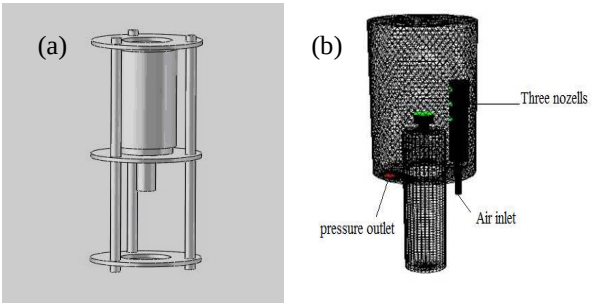

Fig. 1: (a) Combustion chamber (Model 1) with holder frame and (b) computational grid.

Combustion modelling is based on the two-phase Euler-Euler approach which takes into account the interactions of the gaseous and solid phases. The char combustion is considered by the single-step heterogeneous reaction given in equation (1). A user-defined function (UDF), with which the rate of the heterogeneous chemical reaction between the solid and gas phases is defined, and developed and coded in C++ language and incorporated in the solver. Some assumptions are made to simplify the combustion modelling: the solid carbon particles are assumed to be inelastic and monodispersed spheres which represent a pure (100%) carbon. In reality, this is not the case and to some extent the existence of inherent moisture, sulphur, nitrogen, and other non-carbon components will affect combustion characteristics as previously described. Moreover, the virtual mass effect is neglected because the density of the solid phase is greater than that of the gas phase. Since the particle size is small the lift force is not significant and as a result it has also been neglected. Therefore, the interaction between the phases is only due to the drag force.

For the case of 1mm average particle diameter, the volume fraction at different time-steps is shown in Fig. 2. At the beginning the volume fraction was set to 0.6, and the results of the volume fraction of the solid phase taken in the mid-plane of the combustion chamber show them progressing upward with time. Fig. 3 shows the temperature distribution at the different time-steps. It can be seen that the temperature progresses with time, therefore the combustion remains sustained.

Fig. 4 shows the peak temperature with time for three cases with the average particle diameters of 0.5mm, 1 mm and 2mm respectively. It shows that there is an effect of increasing the particle size on the temperature increase and the maximum temperature is obtained with a size of 2 mm.

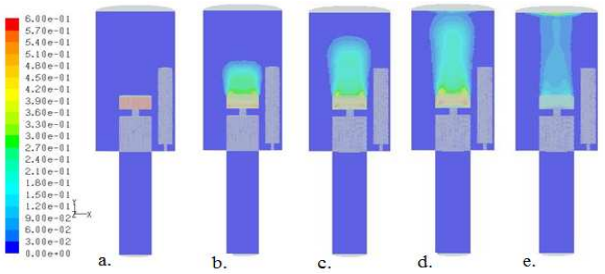

Fig. 2: The variation of solid phase volume fraction at different simulation times (sec): (a) 0, (b) 0.05, (c) 0.1, (d) 0.15 and (e) 0.2.

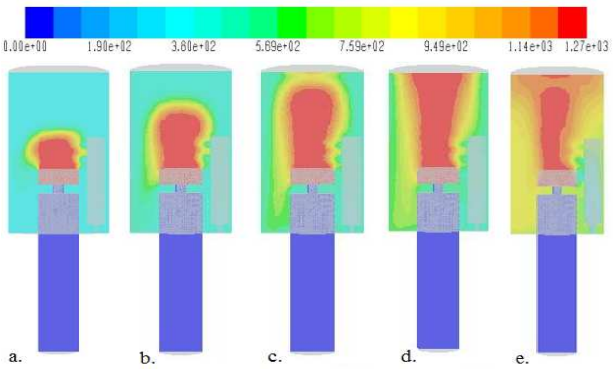

Fig. 3: The variation of temperature at different time steps for 1 mm average particle diameter showing at time (sec): (a) 0, (b) 0.05, (c) 0.1, (d) 0.15 and (e) 0.2.

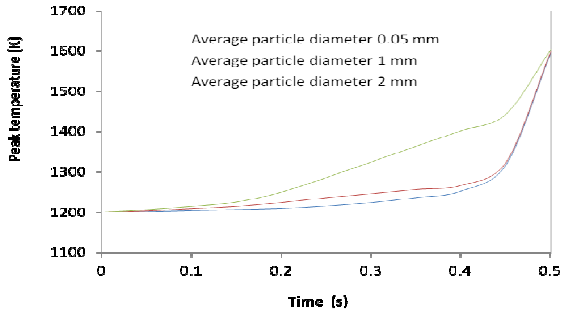

Fig. 4: The peak temperature variation with time for three different particle sizes.

Combustion Model 2

The basic geometry of the reactor considered for this study is taken from Zhang *et al.* [19]. The reactor is 2.5m in length with an internal diameter of 200mm. An axisymmetric computational domain and the burner of the reactor that consists of three concentric tubes are shown in Fig.5. The coal particles are injected centrally through an 8mm diameter inner tube. A concentric tube with a diameter of 18mm makes an annular gap that admits the primary air through it. The secondary air is supplied through another annular gap made by a concentric tube with a diameter of 34mm. The operating conditions are provided in Table 2. Some assumptions are made in order to simplify the modelling: it is assumed that the gas phase can be treated as an ideal-gas mixture and the coal particles are assumed to be spherical in shape and enter the combustor with the same velocity as the carrying air. The temperature of the coal particles is 300K and the side walls are modelled as having a constant temperature maintained by an electrical heater. The interaction between the particles in this case is neglected.

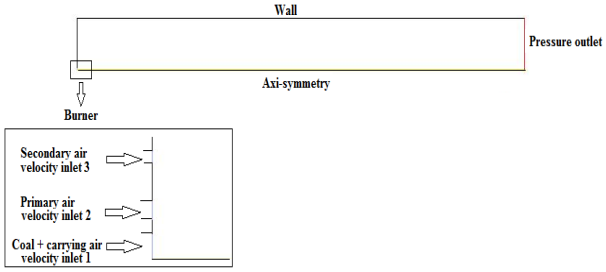

Fig.5. Geometry of the axisymmetric combustor (Model 2).

The model used in this simulation is the discrete phase Eulerian-Lagrangian model. Three cases were simulated: In the first two cases, the char was assumed to be only oxidized to CO_2 according to reaction (1). The char oxidation in the first case (Case 1) was the diffusion model while in the second case (Case 2) was the diffusion-kinetics model. In the third case (Case 3), the combustion of char was assumed to follow the reactions (1-4). To determine the rates of these reactions, UDFs were written and exported to the solver, and the other processes using sub-models are readily available in FLUENT. Furthermore, the particle size distribution of the pulverized coal particles injected into the reactor is assumed to follow a Rosin-Rammler distribution curve based on the assumption that an exponential relationship exists between the particle diameter d_p and the mass fraction of particles Y_d with diameter greater than d_p:

$$Y_d = e^{-(d_p/\bar{d})^n} \quad (8)$$

where ($\bar{d}$) is the mean diameter and (n) is the spread parameter. Six discrete particles have been considered and one way coupling has been assumed. The dispersion of the particles due to turbulence in the gas phase is predicted using a stochastic tracking model.

Table 2: Operating conditions for Model 2

Parameters	Units	Values
Coal mass flow	kg/hr	1
Wall temperature	K	1523
Volume flow rate of coal carrying air	m³/hr	2.38
Temperature of coal carrying air	K	473
Volume flow rate of primary air	m³/hr	4.68
Temperature of primary air	K	523
Volume flow rate of secondary air	m³/hr	11.15
Temperature of secondary air	K	623
Mean diameter of particle	µm	16, 52, 160, 350
Mass fraction of particle diameters	%	30, 35, 25, 10

A steady state computation was initially carried out with a grid resolution having a total of 48000 control volumes. The grid density was reduced and then symmetrically increased to 37500, 52000 and 61000 to check their sensitivity on the results. Fig. 6 shows the temperature inside the reactor along the mid-line for the four grids and the predicted results show reasonably good agreement with small variation at the upstream of the reactor.

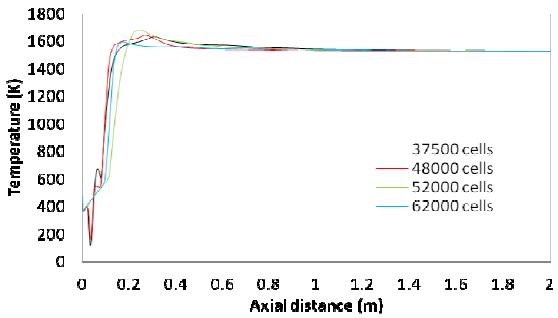

Fig.6. Maximum temperature predicted inside the reactor with different grids.

In order to validate the model, the simulation results are compared with the experiment data of Zhang *et al.* [19] and shown in Figures 7 and 8. It can be seen that the predictions of O_2 and CO_2 concentrations have a good agreement with the experimental data. In

particular, the mass fraction of oxygen along the axial distance of the reactor in Fig. 7 shows the results predicted by Case 3 are closer to the experimental data near the burner than the other two cases, while Case 1 results show better agreement at the exit of the reactor. The mole fractions of carbon dioxide in Fig. 8 also show that the Case 3 results have very good agreement with the experimental data.

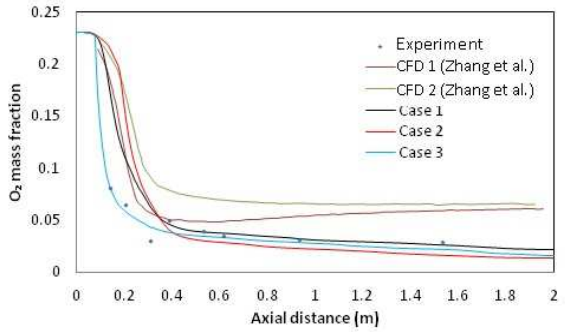

Fig. 7: O_2 mass fraction along the axial distance of the reactor.

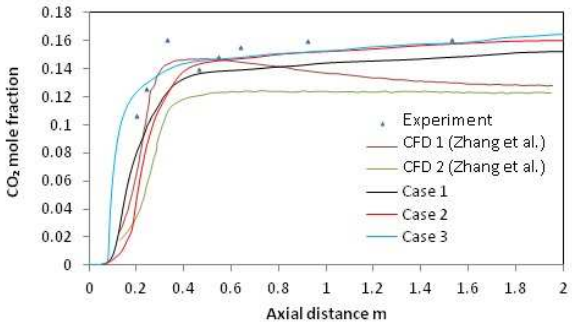

Fig. 8. CO_2 mole fraction along the axial distance of the reactor.

In Fig. 9 it can be seen that there is a flat part of the curves at the beginning for each particle, which means that there is no mass change taking place and the particles only undergo a heating process. It can also be seen that the larger particles need a longer period of time than that of the smaller particles to be heated up. Then, there is a decrease in the mass due to the particle's devolatilization which takes place rapidly for the small particles and becomes slower as the particle size increases.

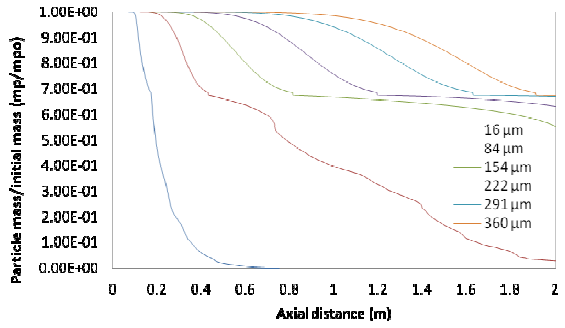

Fig. 9. Mass depletion of particles with different sizes for Case 3.

Conclusion

The heterogeneous combustion of char in biomass and coal combustion is a complex process including the interaction between the gaseous phase and the solid phase. The results in Model 1 show that the combustion was sustained in the chamber, as evidenced by the flame temperature distribution. The temperature was affected by the size of the particles. The second model has been formulated to predict the combustion of pulverized coal. The results showed good agreement with the experimental data. They also showed that the combustion inside the reactor was affected by the particles size. In comparison with the larger particles, it was shown that the volatiles of the smaller particles are released rapidly, and the gas temperature reaches it maximum and then decreases due to the start of endothermic reactions.

The application of biomass combustion and gasification is found in many different types of furnaces such as fixed and moving bed reactors, fluidized or circulating fluidized beds, and pulverized fuel furnaces. Therefore, this study of biomass combustion will not only help to understand its behaviour, but will greatly assist to develop better methods of combustion.

References

[1] C. N. Hamelin, R. A. A. Sours, A. P. C. Fail. International bio energy transport costs and energy balance. Biomass and Bio energy, 2005, 29:114-34.

[2] A. A. Khan, W. D. Jung, P. J. Janssen, H. Spliethoff. Biomass combustion in fluidized bed boilers: Potentials, problems and remedies. Fuel Processing Technology, 2009, 90:21-50.

[3] M. M. Hoodwink, A. P. C. Fail, R. V. D. Broke, G. Bends, D. Gisele, W. C. Turkenburg. Exploration of the ranges of the global potential of biomass for energy. Biomass and Bioenergy, 2003. 25(2):119-33.

[4] V. K. Vera, S. Bram, F. Deleting, P. Lama, I. Vandendael, A. Hubin, J. De Ruyck. Agro-pellets for domestic heating boilers: Standard laboratory and real life performance. Applied Energy, 2011:1-8.

[5] J. Tissari, O. Sippula, J. Kouki, K. Vuorio, J. Jokiniemi. Fine particle and gas emissions from the combustion of agricultural fuels fired in a 20 kW burner. Energy & Fuels, 2008, 22:2033-42.

[6] T. Nussbaumer, Biomass combustion in Europe, overview on technologies and regulations. Report prepared for NYSERDA, April 2008.

[7] P. L. Walker, F. Rusinko, L. G. Austin. Gas reactions of carbon. Advances in catalysis, 1959, 11:133-221.

[8] M. F. Mulcay, I. W. Smith. Kinetics of combustion of pulverized fuel: A review of theory and experiment. Rev.Pure and Appl.Chem., 1969, 19(1):81-108.

[9] R. H. Essenhigh. Combustion and Flame in coal systems. A review. Proc. Combust. Ins.,1976, 16(1):353-374.

[10] R. H. Essenhigh. Fundamentals of coal combustion, In: chemistry of coal utilization, M. A.

Elliott(Ed), Wily-Interscience, New York, pp.1153-1312.
[11] A. Williams, R. Backreedy, J. M. Jones, M. Pourkashanian. Combustion of pulverized coal and biomass. Progress In Energy and combustion science, 2001, 27:587-610.
[12] M. A. Field, D. W. Gill, B. B. Morgan, P. G. W. Hawksley. Combustion of pulverized coal; Leatherhead: England, BCURA, 1967.
[13] S. P. Burke, T. E. W. Schumann. Proceedings of 3rd International Conference on Bituminous Coal, 1932, 2:485-509.
[14] H. Osman, A. Ismail. Numerical analysis of single-particle combustion of coal char, in Mathematical modelling of transport processes. ED, A. P. Samito, S. V. Jangam. Singalore, 1011, 83-108.
[15] D.A. Tillman. The combustion of solid fuels and waste. San Diego: Academic Press, 1991.
[16] J. R. Arthur. Trans Farady Soc, 1951, 42:164.
[17] B. Alganash, M. C. Paul, I. A. Watson. Modelling of heterogeneous combustion processes of biomass. 2013. Submitted for publication.
[18] Fluent 6.3 user's guide, 2005.
[19] Y. Zhang, X. Wei, L. Zhou, H. Sheng. Simulation of coal combustion by turbulence-chemistry char combustion model and a full two-fluid model. Fuel, 2005, 84 :1798-1804.